DOI:10.22059/IJVM.2023.370132.1005499 Iranian Journal of Veterinary Medicine Original Article

Online ISSN: 2252-0554

The Inhibitory Effect of cLF-chimera, a Recombinant Antimicrobial Peptide, on Avian Influenza Virus Subtype H_9N_2

Moein Khodayari[1], Mohammad Hadi Sekhavati[2], Seyed Mostafa Peighambari[1], Abbas Barin[3], Omid Dezfoulian[4], Jamshid Razmyar[1*]

1-Departmen of Avian Diseases, Faculty of Veterinary Medicine, University of Tehran, Tehran, Iran

2-Departmen of Animal Science, Faculty of Agriculture, Ferdowsi University of Mashhad, Mashhad, Iran

3-Departmen of Clinical Pathology, Faculty of Veterinary Medicine, University of Tehran, Tehran, Iran

4-Departmen of Pathobiology, School of Veterinary Medicine, Lorestan University, Khorramabad

Abstract

Background: Avian influenza subtype H9N2 is the most prevalent influenza virus in poultry worldwide. It imposes economic losses on the poultry industry and has zoonotic potential. Currently, there are two main groups of anti-influenza drugs in use; Adamantanes and Neuraminidase inhibitors. In recent years, there has been increasing resistance to existing anti-influenza drugs. Antimicrobial peptides are a group of potential drug candidates with broad-spectrum activity. cLF-chimera is an antimicrobial peptide synthesized from camel milk lactoferrin.

Objectives: This study's objective is to evaluate the inhibitory effects of cLF-chimera on avian influenza, subtype H9N2.

Methods: For this purpose, one hundred and seventy 11-day-old SPF embryonated eggs were randomly distributed in 17 groups. Different virus and peptide concentrations were injected into the eggs. The eggs were incubated for four days with daily candling for viability assessment. On the 4th day of incubation, each group's alive or dead embryos were sorted and evaluated for

gross anomalies. Next, the chick embryos were fixed with 10% neutral buffered formalin for one week for histopathological studies. The MTT assay was also performed for the peptide and virus concentrations.

Results: Overall, the embryo viability results and macroscopic and histopathologic findings showed that the peptide has inhibitory effects against the virus. These findings agree with the MTT assay. Moreover, the peptide has proven effects against pathogenic bacteria that can be advantageous compared to common anti-influenza medications.

Conclusions: According to the results, cLF-chimera has an inhibitory effect on the H9N2 influenza virus.

Keywords

Antimicrobial Peptide; Avian Influenza; cLF-chimera; Histopathology; Subtype H_9N_2

Abbreviations

AIV = avian influenza virus; HA = haemagglutinin; NA = neuraminidase; LPAIV = low pathogenic avian influenza virus; AMP = antimicrobial peptide; HDP = host defense peptide; cLFcin = camel lactoferricin; cLFampin = camel lactoferampin; MDCK = Madin-Darby canine kidney; DMEM = Dulbeco's minimal essential medium; FBS = fetal bovine serum; EID_{50} = embryo infective dose50; CAF = chorioallantoic fluid; HA test = haemagglutination test; H&E =

hematoxylin and eosin; DMSO = Dimethyl sulfoxide; OD = optical density; ELISA = enzyme-linked immunosorbent assay; ANOVA = analysis of variance; CPE = cytopathogenic effect

Introduction

Avian influenza viruses (AIVs) have a negative-sense RNA genome with eight segments in the *Orthomyxoviridae* family and *Influenza A* genus (Perez DR 2019, Mohammadi, Sekhavati *et al.* 2023). They are categorized as high and low pathogenic based on the pathogenicity and molecular markers. They are also classified into 16 HA and 9 NA subtypes based on surface glycoproteins haemagglutinin (HA) and neuraminidase (NA) (Swayne, Suarez *et al.* 2020, Sheykhi, Modirrousta *et al.* 2021). The H_9N_2 subtype is a low pathogenic AIV (LPAIV), which is the most prevalent avian influenza virus in poultry worldwide (Nagy, Mettenleiter *et al.* 2017). Its first report was from turkeys in the USA in 1966 (Nagy, Mettenleiter *et al.* 2017). Later, it spread to Asia, especially in 1990s (Nagy, Mettenleiter *et al.* 2017, Mehrabadi, Ghalyanchilangeroudi *et al.* 2019). The first report on H_9N_2 in Iran was by Vasfi *et al.* in 1998. Since then, the virus has been endemic in Iran and reported frequently (Ahmadi, Rajabi *et al.* 2018).

The H_9N_2 AIV is important for following reasons: **I:** because of direct and indirect economic losses such as mortality, vaccination, and treatment costs (Swayne, Suarez *et al.* 2020); **II:** the possible transmission to humans. The first zoonotic was reported in China in 1998 (Peacock, James *et al.* 2019, Mayahi, Boroomand *et al.* 2021). Fortunately, in humans it is sporadic with low severity, and there has been no report on transmission among the human population, but the

virus can be considered a pandemic candidate (Pusch and Suarez 2018). **III:** the H_9N_2 can be a gene donor. To date, the role of H_9N_2 AIV in the emergence of at least three influenza subtypes, H_5N_1 (Peacock, James *et al.* 2019), H_7N_9 (Lam, Wang *et al.* 2013), and $H_{10}N_8$ (Chen, Yuan *et al.* 2014), has been recognized.

Nowadays, the prevention strategy in poultry is based on vaccination and biosecurity (Shen, Wu *et al.* 2014, Radmehri, Talebi *et al.* 2021, Motamedinasab, Pourbakhsh *et al.* 2023). However, vaccination is the primary strategy, its effectiveness is mainly influenced by the similarity of vaccine and virus HA glycoprotein (Song and Qin 2020). In addition, vaccination in birds with immunosuppressive diseases has no optimal effect (Sharif and Ahmad 2018).

In humans, anti-influenza drugs are used as treatment and prevention (Amarelle, Lecuona *et al.* 2017). The two main types of medicines, Adamantanes and Neuraminidase inhibitors, have been proven in many countries (Koszalka, Tilmanis *et al.* 2017). The mechanisms of action for these drugs are blocking M_2 ion channel and neuraminidase glycoprotein, respectively (Watanabe and Kawaoka 2015).

Vaccination and biosecurity in poultry cannot completely prevent the disease outbreaks. Currently, there is no specific treatment for poultry, and the use of current human anti-influenza drugs are prohibited in many countries (Tsuruoka, Nakajima *et al.* 2017, Ahmadi, Rajabi *et al.*

2018). On the other hand, drug resistance, especially for Adamantanes, has increased in recent years (Hussain, Galvin *et al.* 2017). In addition, prescribing these drugs 48 hours after the onset of symptoms, is not considered effective (Lehnert, Pletz *et al.* 2016). It is therefore required to search for new anti-influenza agents as a drug that can also be used in poultry, that antimicrobial peptides are one of many candidates (Ahmadi, Rajabi *et al.* 2018, De Angelis, Casciaro *et al.* 2021).

Antimicrobial peptides (AMPs) or host defense peptides (HDPs) are small amino acid molecules (usually less than 100 amino acids) that are part of the innate immune system (Kang, Kim *et al.* 2017, Lei, Sun *et al.* 2019). These peptides exist in many organisms (Lei, Sun *et al.* 2019) and have a broad-spectrum effect on bacteria, fungi, and cancer cells (Yeaman and Yount 2003, Ong, Wiradharma *et al.* 2014). The peptides are also an acceptable candidate in preventing and treating viral diseases, with proven antiviral activity against some DNA and RNA viruses (Bahar and Ren 2013).

A group of AMPs is derived from larger proteins. The N-terminal of lactoferrin has hydrophobic and cationic AMPs with antibacterial, antiviral, and anti-fungal activities (Tanhaiean, Azghandi *et al.* 2018, Tanhaieian, Sekhavati *et al.* 2018). Chimeric peptide cLF-chimera is derived from camel milk lactoferrin. The peptide is synthesized from the linkage of

lactoferricin (cLFcin) C-terminus and lactoferampin (cLFampin) N-terminus by a lysine amino acid (Tanhaiean, Azghandi *et al.* 2018, Pirkhezranian, Tahmoorespur *et al.* 2020) and expressed recombinantly in *E. coli* and *L. lactis* (Tanhaiean, Azghandi *et al.* 2018, Tanhaiean, Sekhavati *et al.* 2018). The peptide has an antibacterial effect against *E. coli*, *S.* Enteritidis, *S.* Typhi, *P. aeruginosa*, and *S. aureus in vitro* and *E. coli* and *C. perfringens*, *in vivo* (Daneshmand, Kermanshahi *et al.* 2019, Daneshmand, Kermanshahi *et al.* 2020, Roshanak, Pirkhezranian *et al.* 2020, Tanhaeian, Sekhavati *et al.* 2020).

There are some researches on natural and synthetic AMPs which focus on antiviral drugs in humans and birds. However, most researches concentrate on human pathogens like MERS-CoV, SARS-CoV, HIV, hepatitis C virus, and measles (Zhao, To *et al.* 2020); others have focused on avian pathogens. One of these important potential zoonotic pathogenes is AIV. Different peptides have been tested on different subtypes of AIV, like H_1, H_3, H_5, H_7 (Li, Zhao *et al.* 2011, Zhao, Zhou *et al.* 2016) and H_9N_2 (Rajik, Jahanshiri *et al.* 2009, Arbi, Larbi *et al.* 2022).

In this study, we also decided to predict the interaction of the so-called peptide with its poteantially related receptors (HA, NA and M2 ion channel). In order to accomplish this task, we used computational modeling technique. Computational modeling has the benefits of reducing

wet lab practices costs and minimizing blind experiments (Meng, Zhang *et al.* 2011). On the other hand, molecular docking has been accepted as a modeling technique that could elucidate the interaction between molecules (Pagadala, Syed *et al.* 2017). This method explains ligand and target protein's most favorable binding mode (Tripathi and Bankaitis 2017). Therefore, it can be used in molecular biology and drug design (Meng, Zhang *et al.* 2011, Pagadala, Syed *et al.* 2017).

The objective of this study was to evaluate the probable inhibitory effects of cLFchimera on H_9N_2 subtype of influenza virus to prevent and treat influenza both in humans and poultry. Moreover, computational modeling predicts the interaction between the peptide and the virus surface projections (HA, NA, M_2).

Materials and methods

Virus, cells, and embryonated eggs

Low Pathogenic AIV (LPAIV) strain A/chicken/Iran/UT-Barin/2017 (H9N2) was used in this study. The virus was provided by the Department of Avian Diseases, Faculty of Veterinary Medicine, University of Tehran. Madin-Darby canine kidney (MDCK) cells were purchased from Razi Vaccine & Serum Research Institute, Iran, and maintained in Dulbecco's minimal essential medium (DMEM; Thermo Fisher Scientific corporation; USA), with 10% fetal bovine serum (FBS; Thermo Fisher Scientific corporation; USA) at 37 centigrade degrees and 5% CO_2 atmosphere. Eleven-day-old SPF embryonated eggs were also used to evaluate the possible virus-peptide interactions.

cLF-chimera peptide

The chimeric peptide is derived from camel-milk lactoferrin. It is synthesized from the linkage of cLFcin C-terminus (amino acids 17-30) and cLFampin N-terminus (amino acids 265–284) by a lysine amino acid. There is also a six-aminoacids-histidine tag linked to lactoferampin (Tanhaiean, Azghandi *et al.* 2018, Tanhaieian, Sekhavati *et al.* 2018). Figure 1(A & B) shows the cartoon shape and amino acid sequence of the peptide.

Experimental design

The study was conducted in 6 steps as below:

Titration of the virus by the EID_{50} method

First, a ten-fold dilution of the virus was prepared. Serial dilution continued to 10^{-9}. Then, each dilution was injected into five SPF embryonated eggs. After incubation at 37°C and 75% humidity for 72 hours, the number of live and dead embryos was counted in each group. Then, the chorioallantoic fluid (CAF) of all eggs was harvested. The fluids were evaluated for the presence of the virus by HA test. To increase the accuracy, HA test was performed in duplicate. To reach 10^2, 10^4, and 10^6 EID_{50} of the virus, Reed and Muench method was performed (Villegas 2008).

Injection of the peptide and titrated virus into embryonated eggs

Eleven-day-old SPF embryonated eggs were randomly distributed into 17 groups (each group with ten eggs). After peptide dilutions were prepared (40, 80, and 160 µg) (Torres, Noll *et al.* 2013, Tahmoorespur, Azghandi *et al.* 2020), 0.1 ml of each dilution was mixed with 0.1 ml of the virus dilutions (10^2, 10^4, and 10^6 EID_{50}). The mixture remained at room temperature for 30 minutes. Then, each inoculum was injected into the allantoic sac of embryonated eggs (Tare and

Pawar 2015). There were three groups: positive, negative, and injection control. All treatment groups are summarized in table 1.

Evaluation of macroscopic and histopathologic lesions of the embryos

The eggs were incubated for four days (Arbi, Larbi *et al.* 2022) in a GALLENKAMP® incubator model at 37°C and 75% humidity. During this period, all eggs were daily candled for viability. The deaths in the first 24 hours were assumed as injection error or probable bacterial infection and were eliminated from the results. On the 4th day of incubation, each group's alive or dead embryos were sorted and evaluated for gross anomalies. Next, the chick embryos were fixed with 10% neutral buffered formalin for one week. Finally, 4 µm tissue sections were provided from the whole chick body, including head, thorax, and abdomen contents, then were embedded in paraffin and stained with hematoxylin and eosin (H&E) for microscopic studies.

Cytotoxicity assay

Ninety-six-well culture plates with MDCK cells were incubated at 37 centigrade degrees with a 5% CO_2 atmosphere for a day. Cells were then treated with various concentrations of the peptide, virus, and peptide-treated virus for 24 hours with the same condition of the previous step (Table

2 shows all 14 groups in detail). Next, a cell viability assay was performed by MTT method to determine the cytotoxicity of all the treatment groups. In brief, 10 µL of MTT solution was added to each well and incubated for four hours at 37°C. Then, 50 µL of DMSO solution (Thermo Fisher Scientific corporation; USA) was added to the wells. Finally, the solution's optical density (OD) was measured at 570 nm by ELISA reader (anthos 2020®) (Bahuguna, Khan *et al.* 2017, Mehrbod, Abdalla *et al.* 2018).

Computational modeling

SWISS-MODEL web server modeled the HA, NA, and M_2 projections (Waterhouse, Bertoni *et al.* 2018). PEP-FOLD web server also modeled the peptide (Shen, Maupetit *et al.* 2014). Then, docking complexes, prepared with ClusPro web server (Porter, Xia *et al.* 2017), were opened with Pymol software (Schrödinger L 2020). Afterwards, photos were taken in the ligand-receptor interaction site.

Statistical analysis

Statistical analysis and diagrams were performed by Graph Pad Prism software, version 8.0 (GraphPad Software, Boston, Massachusetts USA, www.graphpad.com). The data represent the

mean±standard deviation for each sample. The two-way analysis of variance (ANOVA) was used to compare the means.

Results

Injection of peptide and titrated virus to embryonated eggs

After four days of incubation, eggs were candled to identify the livability of the embryos. The results showed 100% vitality for all peptide concentrations (CP1, CP2, and CP3). There was also nearly 100% viability in all V1 (V1P1, V1P2, and V1P3) and V2 (V2P1, V2P2, and V2P3) groups (except a death related to injection error in V2P2 group). All embryos in V3P1 and V3P2 were dead, but V3P3 had very high livability (except two deaths related to injection error in V3P3). All embryos were dead in virus control groups (CV1, CV2, and CV3), as expected. Table 3 shows the results in detail.

Macroscopic and histopathologic lesions observed in embryos

After four days of incubation and determining the number of live and dead embryos, they were all checked for visible gross lesions. Based on the findings, the embryos in virus controls (CV1, CV2, CV3), V3P1, and V3P2 were dwarf, featherless, and with visible hemorrhagic lesions in some cases. In contrast, embryos were larger, feathered, and had no visible lesions in the remaining groups (all V1, all V2, and V3P3). Figure 2 shows prominent macroscopic findings in some groups.

After checking for gross lesions, all the embryos were processed and stained with hematoxylin and eosin for microscopic studies. The results showed lesions in different organs in the virus control groups (CV1, CV2, CV3), V3P1, and V3P2. The lesions were more severe in the virus control groups, while no significant histopathologic lesions were observed in other groups. Table 4 and Figure 3(A-G) indicate the histopathological findings in detail.

Histopathologic evaluation demonstrated target organs being affected significantly in CV1, CV2, CV3, V3P1, and V3P2, according to table 4:

The major histopathological findings in brains of control group were included of large vacuolation of neuropil (status spongiosis), which established by edema. Moreover the blood vessels were obviously congested, and ischemic neuronal changes scattered throughout the parenchyma.

Massive hemorrhage and congestion in large and small blood vessels appeared in renal and perirenal adipose tissues. The intensive tubular necrosis with deep eosinophilic staining was an outstanding finding. Glomeruli were relatively spared from influential damage, and the interstitium was invaded by a large population of inflammatory cells, chiefly mononuclear cells. Intensive hemorrhage with focal to diffuse hepatocellular degeneration or necrosis with marked congestion of central veins and small-sized blood vessels and sinusoids were obvious in the liver.

large pulmonary vascular congestion with hemorrhage in the interstitium, which was accompanied by large amounts of inflammatory cells were determined in the pulmonary parenchyma. Furthermore, primitive parabronchi had highly-exfoliated epithelial cells in their lumen.

In the eyeball, the continuous hemorrhages along the choroid layers with extensive edema were striking. Moreover, severe disruption of retinal pigmented epithelium or even in some embryosit completely detached, which not identified in microscopic evaluation. Eventually, hemorrhage and congestion were revealed in dermal and hypodermal layers with degraded collagen fibers in the integument. Other organs with minimal changes were the spleen and intestine, in which the red pulps were filled with erythrocytes in the spleen, and necrotic villi was detected in only some intestinal tissues.

No noticeable changes were observed in other organs like the gizzard, proventriculus, and musculoskeletal system. In peptide or peptide-virus treatment groups, all organs had normal architecture similar to the negative control group. However, mild to moderate congestion was seen in V1P1-3, V2P1-3, and V3P3 groups, and scant infiltration of inflammatory cells were present around central veins with mild hyperplasia of bile ducts in the liver.

Cytotoxicity assay

We have tested different peptide and the virus concentrations and studied the mixtures at 570 nm. The results (Figure 4) showed that the peptide concentration increased in V1 (V1P1, V1P2, and V1P3) and V2 (V2P1, V2P2, and V2P3) groups leading to a decrease in cell viability. All cell viability percentages in V1 groups were lower than V2. In V3 group (V3P1, V3P2, and V3P3), unlike V1 and V2, the increase in the peptide concentration caused an increase in cell viability.

In the peptide controls (CP1, CP2, and CP3), there was a decrease in cell viability with an increase in the peptide amount. The cell viability was the lowest in virus control group (figure 4).

Computational modeling

We have applied SWISS-MODEL and PEP-FOLD web servers to estimate the viral projections and peptide shapes, respectively. Then we used ClusPro web server to evaluate the docking complexes. Figure 5(A&B) shows the docking complexes and putative interactions between receptor and ligand amino acids. Molecular docking showed 5, 7, and 13 possible interactions between the peptide and viral M_2 ion channel, HA, and NA glycoproteins.

Discussion

The H_9N_2 subtype of AIV can cause direct and indirect losses in poultry industry and can be transferred to humans, which is a public health matter (Mostafa, Abdelwhab *et al.* 2018, Ali, Yaqub *et al.* 2019, Perez DR 2019, Swayne, Suarez *et al.* 2020). Because of the highly mutative nature of the virus, resistance to current chemical drugs is a common finding (Jones, Turpin *et al.* 2006). Since chemical drugs have several side effects (Anand, Jacobo-Herrera *et al.* 2019), there is an immediate need for a new group of anti-influenza drugs with less viral resistance and side effects (Sala, Ardizzoni *et al.* 2019). For this purpose, many studies have focused on different drug candidates; one group is antimicrobial peptides which have anti-influenza properties with broad-spectrum activity (Kang, Kim *et al.* 2017). This study evaluated the anti-influenza effects of the novel chimeric peptide, cLF-chimera, on H_9N_2 subtype in embryonated eggs and MDCK cells.

In ovo model is a standard method to evaluate the probable anti-influenza activity of different drug candidates. It is an ethical way in contrast to laboratory animal models and is on the edge of *in vitro* and *in vivo* models (Ghoke, Sood *et al.* 2018). In this study, the data from embryonated egg injection (Table 3) showed that the embryos were highly livable without distinct macroscopic lesions (Figure 2) in peptide control groups. This result is comparable with

Michálek *et al.'s* results that have used melittin as an antimicrobial peptide in 2 µM concentration which did not severely affect embryo vitality, and the embryos did not have macroscopic lesions (Michálek, Zítka *et al.* 2015). In addition, the histopathological findings in peptide control groups were similar to negative control and saline control without any significant changes (Table 4 & Figure 3). Based on the above data, it is inferable that the peptide was not toxic to embryos in given doses.

We have observed that in virus control groups, embryo mortality was 100% (Table 3), and the embryos were dwarf, featherless with visible hemorrhagic lesions in some cases (Figu 2). Knowing that Avian Influenza viruses cause pathological changes in chicken embryos through apoptosis and necrosis (Ahmadi, Rajabi *et al.* 2018), the histopathological findings contribute to the viral damage. In our study, histopathological results in virus control groups revealed that (Table 4 & Figure 3), except for the gastrointestinal tract with minimal lesions, the other main infected organs were prominently affected and severely damaged. This result is comparable with Shah *et al.*'s study who evaluated the potential effect of three herbal extracts on H_9N_2 subtype in embryos. In their study, positive controls were severely damaged in different organs (Liver, spleen, bursa) (Shah, Tipu *et al.* 2021). All in all, it is clear that the virus is very harmful to embryos in given doses.

Our results also revealed that the embryos were very livable in all V1 and all V2 groups (Table 3), without distinct macroscopic lesions (Figure 2). The histopathological findings in all of these groups showed mild lesions in some cases (Table 4 & Figure 3). According to the results, the peptide in given doses in all V1 and V2 groups could prevent the adverse effect of the different virus concentrations *in ovo*. This data (especially embryo survival rate) is comparable with the study by Sauerbrei *et al*. on H_9N_2 subtype (Sauerbrei, Haertl *et al.* 2006). In this research, four anti-influenza drugs were evaluated against 10^2 and 1 EID_{50} units of the virus: Amantadine, Rimantadine, Oseltamivir, and Zanamivir, with the highest embryo survival rate of 21.9% for adamantanes and 50% for neuraminidase inhibitors (Sauerbrei, Haertl *et al.* 2006).

In V3P1 and V3P2 groups, the embryo survival rate is zero (Table 3), and embryos are dwarf, featherless, with apparent macroscopic lesions (like hemorrhagic lesions) in some cases (Figure 2). At histopathology, severe lesions were detected in these groups (like virus controls, but the lesions were less severe, and V3P2 group had less severe lesions than V3P1) (Table 4 & Figure 3). The data also indicated that the low and medium peptide concentrations could not entirely prevent destructive viral effects in the embryos. In V3P3 group, the survival rate is very high (except the deaths due to injection error) (Table 3), and the embryos have no noticeable macroscopic lesions (Figure 2). From the histopathological point of view, the findings are similar

to peptide control, negative control, saline control, and all V1 and V2 groups (Table 4) without any significant changes (Figure 3). Based on the data obtained from V3 groups, it is deducible that the peptide could prevent the adverse effect of the virus in a dose-dependent manner.

MTT is a color-based assay that evaluates the metabolic activity of cells. The assay is routine, easy, and advantageous for different animal cell lines (Tolosa, Donato *et al.* 2015). According to the results obtained from MTT assay in peptide control groups (Figure 4), the cell viability decreases as the peptide dose increases. This result suggests that the peptide is toxic to the cell line in a dose-dependent manner. This data agrees with previous studies on different antiviral peptides for different cell lines (Sala, Ardizzoni *et al.* 2019, De Angelis, Casciaro *et al.* 2021). Overall, our results indicated that the peptide was toxic for the cell line but not for the embryo. This difference can result from lack of defense mechanisms and higher sensitivity of cells in the cell culture system compared to the body (Hartung 2007).

We have also discovered that in the virus control group, the percentage of cell viability was the lowest of all groups (Table 5). The low percentage can be due to cytopathic effects (CPE) of the virus (Chen, Lin *et al.* 2022). Based on the data, it is obvious that both the peptide and the virus harmed cell livability, but the effect of the virus is much higher.

Our study showed that in V1 groups, the cell viability decreases as the peptide dose increases, and V1P1 had the best cell livability (Figure 4). The cell viability percentage of these groups is lower than the same dose of peptide controls, but is higher than virus control (except V1P3 which is higher than P3 alone, but with a minimum difference) (Figure 4). It seems that the peptide in V1P3 group can block the viral effect, and the remaining peptide have lower toxicity than P3 alone. As the viral dose is constant in these groups, it is more probable that the decrease in cell viability is much related to peptide toxicity. Still, at the same time, the peptide can partially prevent the destructive effects of the virus.

The data from V2 groups are similar to that of V1, but all cell viability percentages are higher (Figure 4). As in these groups, like V1, the virus amount is constant; it seems that the decrease in cell vitality is related to peptide toxicity. Compared to the virus control, in V2 groups, the peptide can partially inhibit the harmful effects of the virus.

In V3 groups, our data showed that unlike V1 and V2, the increase in the peptide dose causes an increase in cell viability (Figure 4). All the percentages were higher than the virus control but lower than the peptide controls. Because the virus concentration is constant, and the decrease in V3P1 and V3P2 is much higher than in previous groups and it is close to the virus

control, it might primarily result from viral CPE. However, even in this group, the peptide can partly block the virus's adverse effects.

Based on the data obtained in these three groups, it is inferable that the peptide can inhibit the destructive viral effects in all the groups. Our study also revealed that the optimum dose of the peptide in all V1, V2, and V3 groups were V1P1, V2P1, and V3P3, respectively.

Molecular docking is a drug design procedure that anticipates binding form and mimics the molecular interaction of ligand and receptor (Fan, Fu *et al.* 2019). In our study, we have also evaluated the interaction between the peptide, viral surface glycoproteins (HA and NA), and M_2 ion channel by molecular docking in order to determine the probable mechanism of action for the peptide. According to the docking results (Figire 5), M_2 ion channel has five possible interactions with the peptide. According to the previous studies on Adamantane's action mechanism, amino acid residue ASP-44 is a site of action for these drugs (Rosenberg and Casarotto 2010, Özbil 2019). Thus, the peptide may mimic Adamantane's action mechanism by blocking M_2 ion channel (Figure 5, A&B).

The docking complex between the peptide and viral HA showed seven potential peptide attachment residues. Based on previous researches on drugs that block HA glycoprotein, amino acids ASN-153 and ARG-131 are in the receptor-binding site of HA_1 (Yang, Li *et al.* 2013).

Therefore, the peptide may prevent the attachment of the virus to cellular receptors (Figure 5, C&D).

Our docking results also showed 13 possible interaction sites between the peptide and viral NA glycoprotein (Figure 5, E&F). Based on previous studies on NA blockers, none of these interaction sites have a role in blocking NA glycoprotein. However, as for the high number of potential attachment sites, further studies are required which can be a subject for later studies on cLF-chimera.

Finally, antimicrobial peptides like cLF-chimera can have different potential modes of action. Some action mechanisms include: inhibiting virus attachment and cell membrane fusion, disrupting viral envelope, inhibiting viral replication, and other probable mechanisms (Skalickova, Heger *et al.* 2015). Therefore, the anti-influenza effect of the peptide in this study can be a combination of the mentioned mechanisms.

cLF-chimera has also proven the effects against bacteria participating in respiratory complexes (Tanhaiean, Azghandi *et al.* 2018, Tanhaieian, Sekhavati *et al.* 2018, Roshanak, Pirkhezranian *et al.* 2020, Tanhaeian, Sekhavati *et al.* 2020). This study also suggests that the peptide has potential anti-influenza properties. Since H9N2 subtype can mainly cause respiratory disease in poultry (Nili and Asasi 2003, Swayne, Suarez *et al.* 2020) and flu-like, mild, primarily

respiratory illness in human populations (Liu, Zhao *et al.* 2018, Song and Qin 2020), the peptide can affect the virus and other secondary bacteria. Compared to common anti-influenza drugs, this broad-spectrum impact can be an advantage for the peptide.

In most viral respiratory diseases, a primary viral agent is accompanied by secondary infections (Seto, Conly *et al.* 2013, Swayne, Suarez *et al.* 2020). However, further studies are needed to explain the potential pros and cons of the peptide as a drug candidate. This study elucidates some peptide characteristics with some undefined questions regarding its novelty: how to use the peptide *in vivo*? how to find its precise dosage and what is the exact mechanism of action? These topics are beyond the scope of this papr, but can be evaluated in future studies.

Statement of animal rights

This study was approved by the animal ethics committee of the University of Tehran under approval number IR.UT.VETMED.REC.1401.004.

Conflict of interest statement

The authors state no conflict of interest.

Data Availability

The data sets generated during and/or analysed during the current study are available from the corresponding authors on reasonable request.

References

Ahmadi, S., Z. Rajabi and M. Vasfi-Marandi. (2018) Evaluation of the antiviral effects of aqueous extracts of red and yellow onions (Allium Cepa) against avian influenza virus subtype H9N2. Iran J Vet Sci Technol. 10: 23-27. https://doi.org/10.22067/veterinary.v2i10.74060.

Ali, M., T. Yaqub, N. Mukhtar, M. Imran, A. Ghafoor, M. F. Shahid, M. Naeem, M. Iqbal, G. J. Smith and Y. C. Su. (2019) Avian influenza A (H9N2) virus in poultry worker, Pakistan, 2015. Emerg. Infect. Dis. 25: 136. https://doi.org/10.3201/eid2501.180618.

Amarelle, L., E. Lecuona and J. I. Sznajder. (2017) Anti-influenza treatment: drugs currently used and under development. Arch. Bronconeumol. 53: 19-26. https://doi.org/10.1016/j.arbres.2016.07.004.

Anand, U., N. Jacobo-Herrera, A. Altemimi and N. Lakhssassi. (2019) A comprehensive review on medicinal plants as antimicrobial therapeutics: potential avenues of biocompatible drug discovery. Metabolites. 9: 258. https://doi.org/10.3390/metabo9110258.

Arbi, M., I. Larbi, J. Nsiri, I. El Behi, A. Rejeb, K. Miled, A. Ghram and M. Houimel. (2022) Inhibition of avian influenza virus H9N2 infection by antiviral hexapeptides that target viral attachment to epithelial cells. Virus Res. 313: 198745. https://doi.org/10.1016/j.virusres.2022.198745.

Bahar, A. A. and D. Ren. (2013) Antimicrobial peptides. Pharmaceuticals. 6: 1543-1575. https://doi.org/10.3390/ph6121543.

Bahuguna, A., I. Khan, V. K. Bajpai and S. C. Kang. (2017) MTT assay to evaluate the cytotoxic potential of a drug. Bangladesh J. Pharmacol. 12: 115-118. https://doi.org/10.3329/bjp.v12i2.30892.

Chen, H., H. Yuan, R. Gao, J. Zhang, D. Wang, Y. Xiong, G. Fan, F. Yang, X. Li and J. Zhou. (2014) Clinical and epidemiological characteristics of a fatal case of avian influenza A H10N8 virus infection: a descriptive study. The Lancet. 383: 714-721. https://doi.org/10.1016/S0140-6736(14)60111-2.

Chen, J.-J., P.-H. Lin, Y.-Y. Lin, K.-Y. Pu, C.-F. Wang, S.-Y. Lin and T.-S. Chen. (2022) Detection of Cytopathic Effects Induced by Influenza, Parainfluenza, and Enterovirus Using Deep Convolution Neural Network. Biomedicines. 10: 70. https://doi.org/10.3390/biomedicines10010070.

Daneshmand, A., H. Kermanshahi, M. H. Sekhavati, A. Javadmanesh and M. Ahmadian. (2019) Antimicrobial peptide, cLF36, affects performance and intestinal morphology, microflora, junctional proteins, and immune cells in broilers challenged with E. coli. Sci. Rep. 9: 14176. https://doi.org/10.1038/s41598-019-50511-7.

Daneshmand, A., H. Kermanshahi, M. H. Sekhavati, A. Javadmanesh, M. Ahmadian, M. Alizadeh and A. Aldawoodi. (2020) Effects of cLFchimera peptide on intestinal morphology, integrity, microbiota, and immune cells in broiler chickens challenged with necrotic enteritis. Sci. Rep. 10: 1-11. https://doi.org/10.1038/s41598-020-74754-x.

De Angelis, M., B. Casciaro, A. Genovese, D. Brancaccio, M. Marcocci, E. Novellino, A. Carotenuto, A. Palamara, M. Mangoni and L. Nencioni. (2021) Temporin G, an amphibian antimicrobial peptide against influenza and parainfluenza respiratory viruses: insights into biological activity and mechanism of action. FASEB J. 35: e21358. https://doi.org/10.1096/fj.202001885RR.

Fan, J., A. Fu and L. Zhang. (2019) Progress in molecular docking. Quantitative Biology. 7: 83-89. https://doi.org/10.1007/s40484-019-0172-y.

Ghoke, S., R. Sood, N. Kumar, A. Pateriya, S. Bhatia, A. Mishra, R. Dixit, V. Singh, D. Desai and D. Kulkarni. (2018) Evaluation of antiviral activity of Ocimum sanctum and Acacia arabica leaves extracts against H9N2 virus using embryonated chicken egg model. BMC Complement Altern. Med. 18: 1-10. https://doi.org/10.1186/s12906-018-2238-1.

Hartung, T. (2007) Food for thought... on cell culture. ALTEX-Alternatives to animal experimentation. 24: 143-152. https://doi.org/10.14573/altex.2007.3.143.

Hussain, M., H. D. Galvin, T. Y. Haw, A. N. Nutsford and M. Husain. (2017) Drug resistance in influenza A virus: the epidemiology and management. Infect Drug Resist. 10: 121-134. https://doi.org/10.2147/IDR.S105473.

Jones, J. C., E. A. Turpin, H. Bultmann, C. R. Brandt and S. Schultz-Cherry. (2006) Inhibition of influenza virus infection by a novel antiviral peptide that targets viral attachment to cells. Virol. J. 80: 11960-11967. https://doi.org/10.1128/jvi.01678-06.

Kang, H.-K., C. Kim, C. H. Seo and Y. Park. (2017) The therapeutic applications of antimicrobial peptides (AMPs): a patent review. J. Microbiol. 55: 1-12. https://doi.org/10.1007/s12275-017-6452-1.

Koszalka, P., D. Tilmanis and A. C. Hurt. (2017) Influenza antivirals currently in late-phase clinical trial. Influenza other Respir. Viruses. 11: 240-246. https://doi.org/10.1111/irv.12446.

Lam, T. T.-Y., J. Wang, Y. Shen, B. Zhou, L. Duan, C.-L. Cheung, C. Ma, S. J. Lycett, C. Y.-H. Leung and X. Chen. (2013) The genesis and source of the H7N9 influenza viruses causing human infections in China. Nature. 502: 241-244. https://doi.org/10.1038/nature12515.

Lehnert, R., M. Pletz, A. Reuss and T. Schaberg. (2016) Antiviral medications in seasonal and pandemic influenza: A systematic review. Dtsch Arztebl Int. 113: 799. https://doi.org/10.3238/arztebl.2016.0799.

Lei, J., L. Sun, S. Huang, C. Zhu, P. Li, J. He, V. Mackey, D. H. Coy and Q. He. (2019) The antimicrobial peptides and their potential clinical applications. Am. J. Transl. Res. 11: 3919.

Li, Q., Z. Zhao, D. Zhou, Y. Chen, W. Hong, L. Cao, J. Yang, Y. Zhang, W. Shi and Z. Cao. (2011) Virucidal activity of a scorpion venom peptide variant mucroporin-M1 against measles, SARS-CoV and influenza H5N1 viruses. Peptides. 32: 1518-1525. https://doi.org/10.1016/j.peptides.2011.05.015.
Liu, R., B. Zhao, Y. Li, X. Zhang, S. Chen and T. Chen. (2018) Clinical and epidemiological characteristics of a young child infected with avian influenza A (H9N2) virus in China. J. Int. Med. 46: 3462-3467. https://doi.org/10.1177/0300060518779959.
Mayahi, M., Z. Boroomand and A. Shoshtari. (2021) Avian Influenza-Killed Vaccine on Tissue Distribution and Shedding of Avian Influenza Virus H9N2 in Ducklings. Archives of Razi Institute. 76: 437.
Mehrabadi, M. H. F., A. Ghalyanchilangeroudi, M. H. Rabiee and F. Tehrani. (2019) Prevalence and risk factors of avian influenza H9N2 among backyard birds in Iran in 2015. Asian Pac. J. Trop. Med. 12: 559. https://doi.org/10.4103/1995-7645.272486.
Mehrbod, P., M. A. Abdalla, E. M. Njoya, A. S. Ahmed, F. Fotouhi, B. Farahmand, D. A. Gado, M. Tabatabaian, O. G. Fasanmi and J. N. Eloff. (2018) South African medicinal plant extracts active against influenza A virus. BMC Complement Altern. Med. 18: 1-10. https://doi.org/10.1186/s12906-018-2184-y.
Meng, X.-Y., H.-X. Zhang, M. Mezei and M. Cui. (2011) Molecular docking: a powerful approach for structure-based drug discovery. Curr Comput Aided Drug Des. 7: 146-157. https://doi.org/10.2174/157340911795677602.
Michálek, P., O. Zítka, R. Guráň, V. Milosavljevič, P. Kopel, V. Adam and Z. Hegar (2015). Effect of melittin on influenza-infected chicken embryos, MendelNet.
Mohammadi, E., M. H. Sekhavati, Z. Pirkhezranian, N. Shafizade, S. Dashti and N. Saedi. (2023) Designing and Computational Analysis of Chimeric Avian Influenza Antigen: A Yeast-Displayed Universal and Cross-Protective Vaccine Candidate. Journal of poultry sciences and avian diseases.
Mostafa, A., E. M. Abdelwhab, T. C. Mettenleiter and S. Pleschka. (2018) Zoonotic potential of influenza A viruses: a comprehensive overview. Viruses. 10: 497. https://doi.org/10.3390/v10090497.
Motamedinasab, S. I., S. A. Pourbakhsh and H. H. Nazarpak. (2023) Evaluation of inactivated vaccine's Antibody response to different H9N2 Vaccination programs with Hemagglutination Inhibition (HI) assay. Journal of poultry sciences and avian diseases
Nagy, A., T. Mettenleiter and E. Abdelwhab. (2017) A brief summary of the epidemiology and genetic relatedness of avian influenza H9N2 virus in birds and mammals in the Middle East and North Africa. Epidemiol. Infect. 145: 3320-3333. https://doi.org/10.1017/S0950268817002576.
Nili, H. and K. Asasi. (2003) Avian influenza (H9N2) outbreak in Iran. Avian Dis. 47: 828-831. https://doi.org/10.1637/0005-2086-47.s3.828.

Ong, Z. Y., N. Wiradharma and Y. Y. Yang. (2014) Strategies employed in the design and optimization of synthetic antimicrobial peptide amphiphiles with enhanced therapeutic potentials. Adv. Drug Deliv. Rev. 78: 28-45. https://doi.org/10.1016/j.addr.2014.10.013.
Özbil, M. (2019) Computational investigation of influenza A virus M2 protein inhibition mechanism by ion channel blockers. Turk. J. Chem. 43: 335-351. https://doi.org/10.3906/kim-1805-39.
Pagadala, N. S., K. Syed and J. Tuszynski. (2017) Software for molecular docking: a review. Biophys. Rev. 9: 91-102. https://doi.org/10.1007/s12551-016-0247-1.
Peacock, T. P., J. James, J. E. Sealy and M. Iqbal. (2019) A global perspective on H9N2 avian influenza virus. Viruses. 11: 620. https://doi.org/10.3390/v11070620.
Perez DR, C. S., Cardenas-Garcia S, Ferreri LM., Santos J, Rajao DS. , Poole. (2019) Avian Influenza Virus. Samal SK (ed) Avian Virology current research and future trends. Caister Academic Press. 1-41.
Pirkhezranian, Z., M. Tahmoorespur, X. Daura, H. Monhemi and M. H. Sekhavati. (2020) Interaction of camel Lactoferrin derived peptides with DNA: a molecular dynamics study. BMC Genom. 21: 1-14. https://doi.org/10.1186/s12864-020-6458-7.
Porter, K. A., B. Xia, D. Beglov, T. Bohnuud, N. Alam, O. Schueler-Furman and D. Kozakov. (2017) ClusPro PeptiDock: efficient global docking of peptide recognition motifs using FFT. Bioinformatics. 33: 3299-3301. https://doi.org/10.1093/bioinformatics/btx216.
Pusch, E. A. and D. L. Suarez. (2018) The multifaceted zoonotic risk of H9N2 avian influenza. Vet. Sci. 5: 82. https://doi.org/10.3390/vetsci5040082.
Radmehri, M., A. Talebi, M. Gholipour and M. Taghizadeh. (2021) Comparative study on the efficacy of MF 59, ISA70 VG, and nano-aluminum hydroxide adjuvants, alone and with nano-selenium on humoral immunity induced by a bivalent newcastle+ avian influenza vaccine in chickens. Archives of Razi Institute. 76: 1213.
Rajik, M., F. Jahanshiri, A. R. Omar, A. Ideris, S. S. Hassan and K. Yusoff. (2009) Identification and characterisation of a novel anti-viral peptide against avian influenza virus H9N2. Virology journal. 6: 1-12. https://doi.org/10.1186/1743-422X-6-74.
Rosenberg, M. R. and M. G. Casarotto. (2010) Coexistence of two adamantane binding sites in the influenza A M2 ion channel. Proc. Natl. Acad. Sci. 107: 13866-13871. https://doi.org/10.1073/pnas.1002051107.
Roshanak, S., Z. Pirkhezranian, F. Shahidi and M. hadi Sekhavati. (2020) Antibacterial activity of cLFchimera and its synergistic potential with antibiotics against some foodborne pathogens bacteria. https://doi.org/10.21203/rs.3.rs-31015/v1.

Sala, A., A. Ardizzoni, T. Ciociola, W. Magliani, S. Conti, E. Blasi and C. Cermelli. (2019) Antiviral activity of synthetic peptides derived from physiological proteins. Intervirology. 61: 166-173. https://doi.org/10.1159/000494354.
Sauerbrei, A., A. Haertl, A. Brandstaedt, M. Schmidtke and P. Wutzler. (2006) Utilization of the embryonated egg for in vivo evaluation of the anti-influenza virus activity of neuraminidase inhibitors. Med. Microbiol. Immunol. 195: 65-71. https://doi.org/10.1007/s00430-005-0002-x.
Schrödinger L, D. W. (2020) PyMOL. Retrieved from http://www.pymol.org/pymol.
Seto, W., J. Conly, C. Pessoa-Silva, M. Malik and S. Eremin. (2013) Infection prevention and control measures for acute respiratory infections in healthcare settings: an update. East. Mediterr. Health J. 19 Suppl 1: S39-47.
Shah, S., M. Tipu, A. Aslam, A. Khan, M. Shafee, S. Khan, N. Khan and A. Akbar. (2021) RESEARCH ARTICLE Elucidating antiviral activity of Curcuma longa against H9 N2 influenza virus using embryonated chicken egg model. Trop. Biomed. 38: 353-359.
Sharif, A. and T. Ahmad. (2018) Preventing vaccine failure in poultry flocks. Immun-Vaccine Adjuv Deliv Syst Strateg.
Shen, H., B. Wu, G. Li, F. Chen, Q. Luo, Y. Chen and Q. Xie. (2014) H9N2 subtype avian influenza viruses in China: current advances and future perspectives. Hosts and Viruses. 1: 54.
Shen, Y., J. Maupetit, P. Derreumaux and P. Tufféry. (2014) Improved PEP-FOLD approach for peptide and miniprotein structure prediction. J. Chem. Theory Comput. 10: 4745-4758. https://doi.org/10.1021/ct500592m.
Sheykhi, N., H. Modirrousta, N. B. Gh, M. Vasfimarandi and S. Fereidouni. (2021) Surveillance of highly pathogenic avian influenza viruses (H5Nx subtypes) in wild birds in Iran, 2014-2019. Archives of Razi Institute. 76: 487.
Skalickova, S., Z. Heger, L. Krejcova, V. Pekarik, K. Bastl, J. Janda, F. Kostolansky, E. Vareckova, O. Zitka and V. Adam. (2015) Perspective of use of antiviral peptides against influenza virus. Viruses. 7: 5428-5442. https://doi.org/10.3390/v7102883.
Song, W. and K. Qin. (2020) Human-infecting influenza A (H9N2) virus: A forgotten potential pandemic strain? Zoonoses and public health. 67: 203-212. https://doi.org/10.1111/zph.12685.
Swayne, D. E., D. L. Suarez and L. D. Sims (2020). Influenza. Diseases of Poultry: 210-256.
Tahmoorespur, M., M. Azghandi, A. Javadmanesh, Z. Meshkat and M. H. Sekhavati. (2020) A novel chimeric anti-HCV peptide derived from camel lactoferrin and molecular level insight on its interaction with E2. Int J Pept Res Ther. 26: 1593-1605.

Tanhaeian, A., M. H. Sekhavati and M. Moghaddam. (2020) Antimicrobial activity of some plant essential oils and an antimicrobial-peptide against some clinically isolated pathogens. Chem. Biol. Technol. Agric. 7: 1-11. https://doi.org/10.1186/s40538-020-00181-9.
Tanhaiean, A., M. Azghandi, J. Razmyar, E. Mohammadi and M. H. Sekhavati. (2018) Recombinant production of a chimeric antimicrobial peptide in E. coli and assessment of its activity against some avian clinically isolated pathogens. Microb. Pathog. 122: 73-78. https://doi.org/10.1016/j.micpath.2018.06.012.
Tanhaieian, A., M. H. Sekhavati, F. S. Ahmadi and M. Mamarabadi. (2018) Heterologous expression of a broad-spectrum chimeric antimicrobial peptide in Lactococcus lactis: its safety and molecular modeling evaluation. Microb. Pathog. 125: 51-59. https://doi.org/10.1016/j.micpath.2018.09.016.
Tare, D. S. and S. D. Pawar. (2015) Use of embryonated chicken egg as a model to study the susceptibility of avian influenza H9N2 viruses to oseltamivir carboxylate. J. Virol. Methods. 224: 67-72. https://doi.org/10.1016/j.jviromet.2015.08.009.
Tolosa, L., M. T. Donato and M. J. Gómez-Lechón. (2015) General cytotoxicity assessment by means of the MTT assay. Protocols in in vitro hepatocyte research. 1250: 333-348. https://doi.org/10.1007/978-1-4939-2074-7_26.
Torres, N. I., K. S. Noll, S. Xu, J. Li, Q. Huang, P. J. Sinko, M. B. Wachsman and M. L. Chikindas. (2013) Safety, formulation and in vitro antiviral activity of the antimicrobial peptide subtilosin against herpes simplex virus type 1. Probiotics Antimicrob. 5: 26-35. https://doi.org/10.1007/s12602-012-9123-x.
Tripathi, A. and V. A. Bankaitis. (2017) Molecular docking: from lock and key to combination lock. J. Mol. Med. 2. https://doi.org/10.16966/2575-0305.106.
Tsuruoka, Y., T. Nakajima, M. Kanda, H. Hayashi, Y. Matsushima, S. Yoshikawa, M. Nagata, H. Koike, C. Nagano and K. Sekimura. (2017) Simultaneous determination of amantadine, rimantadine, and memantine in processed products, chicken tissues, and eggs by liquid chromatography with tandem mass spectrometry. J. Chromatogr. B. 1044: 142-148. https://doi.org/10.1016/j.jchromb.2017.01.014.
Villegas, P. (2008) Titration of biological suspensions, p 217–221. A laboratory manual for the isolation, identification, and characterization of avian pathogens. American Association of Avian Pathologists, Kennett Square, PA.
Watanabe, T. and Y. Kawaoka. (2015) Influenza virus–host interactomes as a basis for antiviral drug development. Curr. Opin. Virol. 14: 71-78. https://doi.org/10.1016/j.coviro.2015.08.008.
Waterhouse, A., M. Bertoni, S. Bienert, G. Studer, G. Tauriello, R. Gumienny, F. T. Heer, T. A. P. de Beer, C. Rempfer and L. Bordoli. (2018) SWISS-MODEL: homology modelling of protein structures and complexes. Nucleic Acids Res. 46: W296-W303. https://doi.org/10.1093/nar/gky427.

Yang, J., M. Li, X. Shen and S. Liu. (2013) Influenza A virus entry inhibitors targeting the hemagglutinin. Viruses. 5: 352-373. https://doi.org/10.3390/v5010352.
Yeaman, M. R. and N. Y. Yount. (2003) Mechanisms of antimicrobial peptide action and resistance. Pharmacol. Rev. 55: 27-55. https://doi.org/10.1124/pr.55.1.2.
Zhao, H., K. K. To, K.-H. Sze, T. T.-M. Yung, M. Bian, H. Lam, M. L. Yeung, C. Li, H. Chu and K.-Y. Yuen. (2020) A broad-spectrum virus-and host-targeting peptide against respiratory viruses including influenza virus and SARS-CoV-2. Nat. Commun. 11: 4252. https://doi.org/10.1038/s41467-020-17986-9.
Zhao, H., J. Zhou, K. Zhang, H. Chu, D. Liu, V. K.-M. Poon, C. C.-S. Chan, H.-C. Leung, N. Fai and Y.-P. Lin. (2016) A novel peptide with potent and broad-spectrum antiviral activities against multiple respiratory viruses. Sci. Rep. 6: 1-13. https://doi.org/10.1038/srep22008.

اثر بازدارندگی cLF-chimera، یک پپتید ضدمیکروب نوترکیب، بر ویروس آنفلوانزای پرندگان، تحت تیپ H_9N_2

معین خدایاری[1]، محمدهادی سخاوتی[2]، سیدمصطفی پیغمبری[1]، عباس برین[3]، امید دزفولیان[4]، جمشید رزم یار[1*]

1. گروه بیماری‌های پرندگان، دانشکده دامپزشکی دانشگاه تهران، تهران، ایران

2. گروه علوم دامی، دانشکده کشاورزی دانشگاه فردوسی، مشهد، ایران

3. گروه کلینیکال پاتولوژی، دانشکده دامپزشکی دانشگاه تهران، تهران، ایران

4. گروه پاتوبیولوژی، دانشکده دامپزشکی دانشگاه لرستان، خرم‌آباد، ایران

چکیده فارسی

زمینه مطالعه: ویروس آنفلوانزای پرندگان تحت تیپ H_9N_2 شایع‌ترین تحت تیپ ویروس آنفلوانزا در ماکیان سراسر جهان است. این تحت تیپ باعث ایجاد ضررهای اقتصادی به صنعت پرورش ماکیان شده و قابلیت سرایت به انسان را دارد. در حال حاضر 2 گروه عمده داروهای ضدآنفولانزا یعنی آدامانتان‌ها و مهار کننده‌های نورآمینیداز برای درمان این تحت تیپ در حال استفاده هستند. پپتیدهای ضدمیکروب که در سالیان اخیر استفاده از آن‌ها به دلیل مقاومت نسبت به داروهای ضد آنفلوانزا رو به افزایش بوده‌است، دسته‌ای از ترکیبات کاندید احتمالی برای درمان آنفولانزا با طیف اثر وسیع هستند. cLF-chimera یک پپتید ضدمیکروب است که از لاکتوفرین شیر شتر سنتز شده‌است.

هدف: هدف این مطالعه بررسی اثرات بازدارندگی cLF-chimera بر روی تحت تیپ H9N2 ویروس آنفلوانزای پرندگان می‌باشد.

روش کار: برای این منظور 170 عدد تخم‌مرغ جنین‌دار 11 روزه SPF به طور تصادفی در 17 گروه توزیع شدند. غلظت‌های مختلف پپتید و ویروس به تخم‌مرغ‌ها تزریق شده و تخم‌مرغ‌ها به مدت 4 روز همراه با کندلینگ روزانه به منظور بررسی میزان زنده‌مانی جنین‌ها انکوبه شدند. در روز چهارم، جنین‌های زنده و مرده در هر گروه جدا شده و از لحاظ وجود ضایعات ماکروسکوپیک ارزیابی شدند. سپس برای مطالعات هیستوپاتولوژیک، جنین‌ها به مدت یک هفته در فرمالین 10% نگهداری شدند. همچنین تست MTT هم برای غلظت‌های مختلف ویروس و پپتید انجام شد.

نتایج: روی هم رفته نتایج مربوط به درصد زنده‌مانی جنین‌ها، ارزیابی‌های ماکروسکوپیک و هیستوپاتولوژیک نشان دادند که پپتید دارای اثرات بازدارندگی علیه ویروس می‌باشد. این نتایج با نتایج حاصل از تست MTT تاییدشدند. علاوه‌براین، پپتید دارای اثرات ضدمیکروبی علیه باکتری‌های پاتوژن می‌باشد که در مقایسه با داروهای ضد آنفلوانزای رایج می‌تواند به عنوان یک مزیت درنظر گرفته‌شود.

نتیجه گیری نهایی: طبق نتایج ذکرشده، cLF-chimea دارای اثر بازدارندگی علیه ویروس آ آنفلوانزای تحت تیپ H9N2 می‌باشد.

کلیدواژه‌ها: آنفلوانزای پرندگان؛ پپتید ضدمیکروب؛ تحت تیپ H9N2؛ هیستوپاتولوژی؛ cLF-chimera

Tables

Table 1: All groups of embryonated egg injection.

Groups	Treatment
C	No treatment for egg control
CS	Normal saline injection for injection shock control

CV1	10^2 EID_{50} unit of the virus injection for virus control
CV2	10^4 EID_{50} unit of the virus injection for virus control
CV3	10^6 EID_{50} unit of the virus injection for virus control
CP1	Control for 40 µg of the peptide
CP2	Control for 80 µg of the peptide
CP3	Control for 160 µg of the peptide
V1P1	10^2 EID_{50} unit of the virus + 40 µg of the peptide
V1P2	10^2 EID_{50} unit of the virus + 80 µg of the peptide
V1P3	10^2 EID_{50} unit of the virus + 160 µg of the peptide
V2P1	10^4 EID_{50} unit of the virus + 40 µg of the peptide
V2P2	10^4 EID_{50}unit of the virus + 80 µg of the peptide
V2P3	10^4 EID_{50}unit of the virus + 160 µg of the peptide
V3P1	10^6 EID_{50} unit of the virus + 40 µg of the peptide
V3P2	10^6 EID_{50} unit of the virus + 80 µg of the peptide
V3P3	10^6 EID_{50} unit of the virus + 160 µg of the peptide

Table 2: All groups of cell culture system.

Groups	Treatment
C	No treatment for cell control
CV	Control of the virus (10^6 EID_{50})
CP1	Control for 40 µg of the peptide
CP2	Control for 80 µg of the peptide
CP3	Control for 160 µg of the peptide
V1P1	10^2 EID_{50} unit of the virus + 40 µg of the peptide

V1P2	10^2 EID_{50} unit of the virus + 80 µg of the peptide
V1P3	10^2 EID_{50} unit of the virus + 160 µg of the peptide
V2P1	10^4 EID_{50} unit of the virus + 40 µg of the peptide
V2P2	10^4 EID_{50} unit of the virus + 80 µg of the peptide
V2P3	10^4 EID_{50} unit of the virus + 160 µg of the peptide
V3P1	10^6 EID_{50} unit of the virus + 40 µg of the peptide
V3P2	10^6 EID_{50} unit of the virus + 80 µg of the peptide
V3P1	10^6 EID_{50} unit of the virus + 160 µg of the peptide

Table 3: Number of live and dead embryos in each group.

Groups	Number of live embryos	Number of dead embryos	Livability (percent)
C	10	0	100
CS	10	0	100
CV1	0	10	0
CV2	0	10	0
CV3	0	10	0
CP1	10	0	100
CP2	10	0	100
CP3	10	0	100
V1P1	10	0	100
V1P2	10	0	100
V1P3	10	0	100
V2P1	10	0	100
V2P2	9	1	90
V2P3	10	0	100
V3P1	0	10	0

V3P2	0	10	0
V3P3	8	2	80

Table 4: Histopathological lesions of the groups. V: Virus: 3 to 1 maximum to minimum concentration (3: High concentration, 2: Medium concentration, 1: Low concentration), C: Control, P: peptide: 3 to 1 maximum to minimum concentration (3: High concentration, 2: Medium concentration, 1: Low concentration), Pathologic observation: (3: Intensive, 2: Moderate, 1: Mild, 0: none)

Tissue/Group	C	CS	CV1	CV2	CV3	CP1	CP2	CP3	V1P1	V1P2	V1P3	V2P1	V2P2	V2P3	V3P1	V3P2	V3P3
CNS	0	0	3	3	3	0	0	0	1	1	0	1	1	0	3	2	0
Eyeball	1	0	3	3	3	1	0	1	2	1	1	1	1	0	3	2	0
Lung	0	0	3	3	3	0	0	0	1	0	0	1	0	0	3	3	0
Liver	0	0	3	3	3	0	0	0	0	0	0	0	0	0	3	3	0
Kidney	0	0	3	3	3	0	0	0	0	0	0	0	0	0	3	3	0
Skin	0	0	3	3	3	0	0	0	1	0	0	0	1	0	3	2	1
Proventriculus	0	0	0	1	1	0	0	0	0	0	0	0	0	0	0	0	0
Intestine	0	1	0	1	1	0	0	0	0	0	0	0	0	0	3	2	0
Spleen	0	0	3	3	3	0	0	0	1	1	1	0	0	0	3	2	1

Figure Legends

Figure 1(A): The cartoon structure of cLFchimera (Green: cLFampin, Orange: Lysine, Blue: cLFcin, Red: Histidine tag) **Figure 1(B):** The sequence of the peptide

Figure 2: Prominent macroscopic findings of the embryos (**A:** C, **B:** CV3, **C:** CP3, **D:** V1P1, **E:** V2P1, **F:** V3P3)

Figure 3: Histopathological lesions in some groups

Figure 3(A): C & CS groups; normal structures of chicken embryo. Brain; the neuropil is intact (a). Eyeball; in the choroid layer, a few thin-walled vessels are congested. RPE (retinal pigmented epithelium) is continuously preserved. (b). Lung; primitive parabronchi (PB) with cuboidal epithelium are embedded in slightly alveolar (loose fibrous) connective tissue (c). Liver; large blood vessels and sinusoids are clear and only a few of vessels in lesser extent congested (d). Kidney; the glomeruli and tubules are in normal conditions, and some blood vessels are congested (e). Skin; normal architecture of feather follicles and epidermal-dermal structure (f). HE. Scale bar (a-f) 400 µm.

Figure 3(B): Virus control groups (CV1, CV2, CV3); Brain; status spongiosis of neuropil (Vacoulation). Blood vessels are intensively congested. The prevascular spaces are significantly extended by edema (arrows) (a). Eyeball; the retinal pigmented epithelial layer (RPE) is

completely detached, and the choroid is extensively congested and hemorrhagic (arrows) (b). Lung; intensive vascular congestion of the vessels and accumulation of both red blood cells and inflammatory cells in parenchyma. The epithelial cells of parabronchi are largely desquamated into the lumen (arrows) (c). Liver; massive congestion of central veins and hemorrhage in parenchyma (arrows). The spaces of Disse are impacted with erythrocytes and focal areas of hepatocellular degeneration or necrosis are evident (d). Kidney; renal disruption with intensive hemorrhage in parenchyma and perirenal tissue (H) along with necrosis of tubular epithelial cells which are markedly hyalinized (arrows). The Large focal population of inflammatory cells are present (asterisks). Scant degeneration of glomeruli (g) are identified (e). Skin; widespread bleeding and congestion of the vessels in the dermis with prominently mononuclear cells infiltration (f). HE. Scale bar a 150 & (b-f) 400 µm.

Figure 3(C): Protein control groups (CP1, CP2, CP3), Brain; normal architecture of neuropil (a). Eyeball: a few micro-vessels are in the choroid layer engorged with erythrocytes (arrow). The retinal pigmented epithelial layer (RPE) is intact (arrowheads) (b). Lung; parabronchi are normal, and Some vessels are markedly congested (c). Liver; the structure is obviously normal. A few central veins are dilated (d). Kidney; normal renal structure with large thin-walled

congested blood vessels (e). Skin; normal anatomy of epidermal-dermal layer (f). HE. Scale bar (A-F) 400 µm.

Figure 3(D): Virus-Protein groups (V1P1, V1P2, V1P3); intact and normal structures of all histological specimens. Brain (a), Eyeball (b), Lung (c), Liver (d), Kidney (e), and Skin (f). HE. Scale bar (a-f) 400 µm.

Figure 3(E): Virus-Protein groups (V2P1, V2P2, V2P3); all tissue structures in normal position. Brain (a), Eyeball (b), lung (c), Liver (d), Kidney (e), and Skin (f). HE. Scale bar (a-f) 400 µm.

Figure 3(F): Virus-Protein groups (V3P1 & V3P2); Brain; status spongiosis of neuropil. Marked congestion of small and medium-sized blood vessels with relatively large perivascular edematous spaces (a). Eyeball; the choroid is extremely widened with a large amount of edema. In the outermost choroid layer, a chain structure of microvessels is highly congested, and the retinal pigmented epithelium is strongly disrupted (b). Lung; disorganized architecture of pulmonary parenchyma. The parabronchi epithelial lining is necrotic and exfoliated into the lumen. Interstitial tissue is invaded by inflammatory and red blood cells, and most air capillaries and vessels are congested (c). Liver; extensive hemorrhage in parenchyma and severe congestion from Disse spaces to large blood vessels. Also, a lesser population of inflammatory cells

amongst erythrocytes are dispersed in the parenchyma (d). Kidney; massive necrosis of tubular cells, that designated as intense eosinophilic structures (e). Skin; tiny to large blood vessels are highly impacted with red blood cells and hemorrhage admixed with inflammatory cells, principally lying at the dermal-epidermal junction. Collagen fibers are degenerated in the deep dermal layer (f). HE. Scale bar (A-F) 400 µm.

Figure 3(G): Virus-Protein group (V3P3); the normal histological architecture of all the organs is demonstrated. Only mild to moderate congestion in the Liver (d), Kidney (e), and Skin (f). Brain (a), Eyeball (b), and Lung (c). HE. Scale bar (A-F) 400 µm

Figure 4: Cell viability in different groups correlated to peptide and virus concentrations (*: $P < 0.05$; ****: $P < 0.00001$, ns: $P > 0.05$)

Figure 5(A): The results of molecular docking between the peptide, the virus M_2 ion channel, and HA glycoprotein. (A & B: M_2 ion channel; Green: The M_2 ion channel, Deep green:

Amino acid residues of M_2 at interaction site, Violet: The peptide, Deep blue: Amino acid residues of the peptide at interaction site; C & D: HA glycoprotein; Cyan: The HA glycoprotein, Green: Amino acid residues of HA at interaction site, Violet: The peptide, Deep blue: Amino acid residues of the peptide at interaction site)

Figure 5(B): The results of molecular docking between the peptide and the virus NA glycoprotein. (E & F: Wheat: The NA glycoprotein, Deep pink: Amino acid residues of NA at interaction site, Violet: The peptide, Deep blue: Amino acid residues of the peptide at interaction site)

Figures

Figure 1(A)

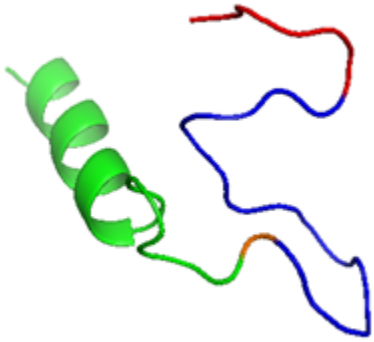

Figure 1(B)

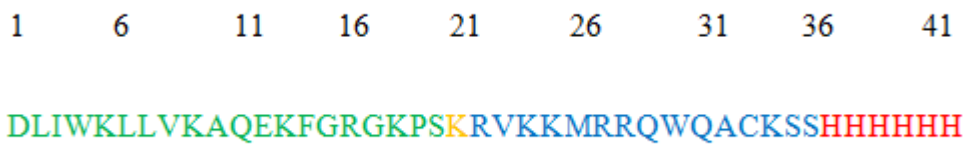

Figure 2

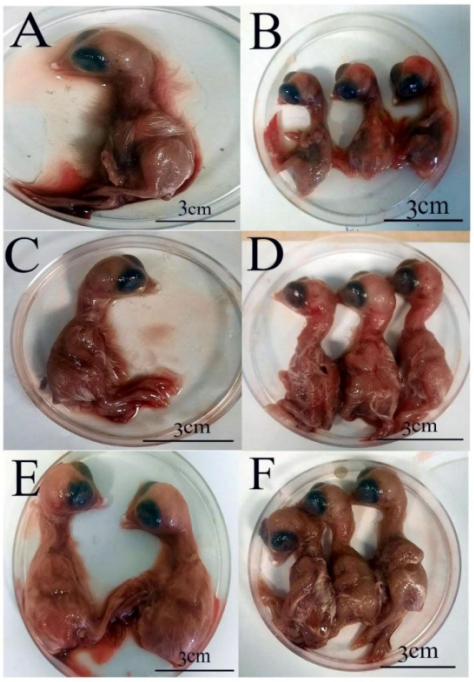

Figure 3(A)

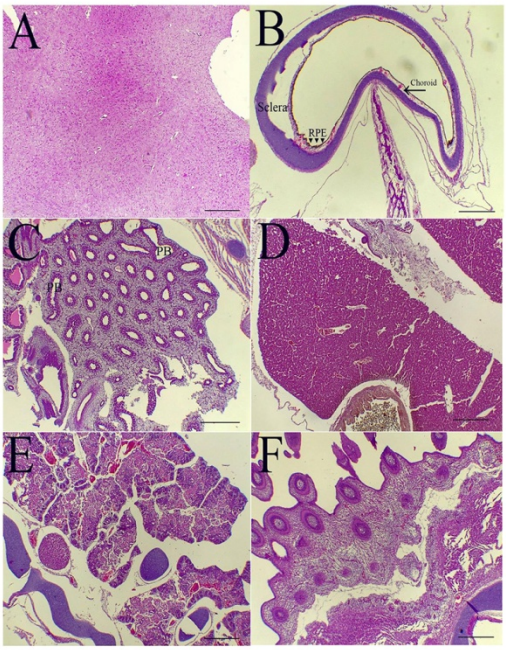

Figure 3(B)

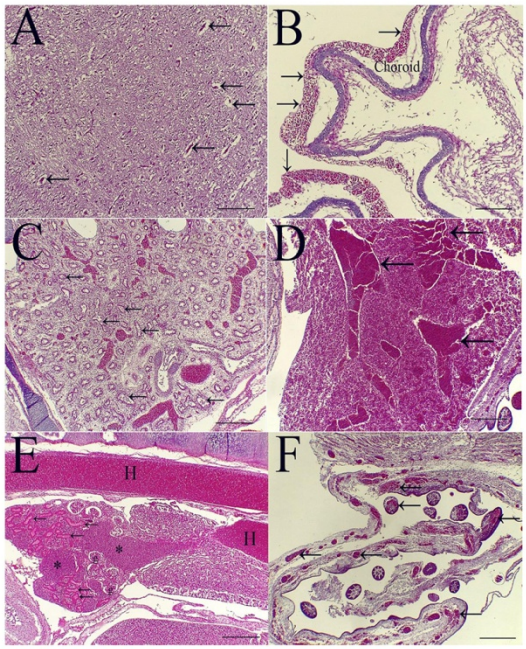

Figure 3(C)

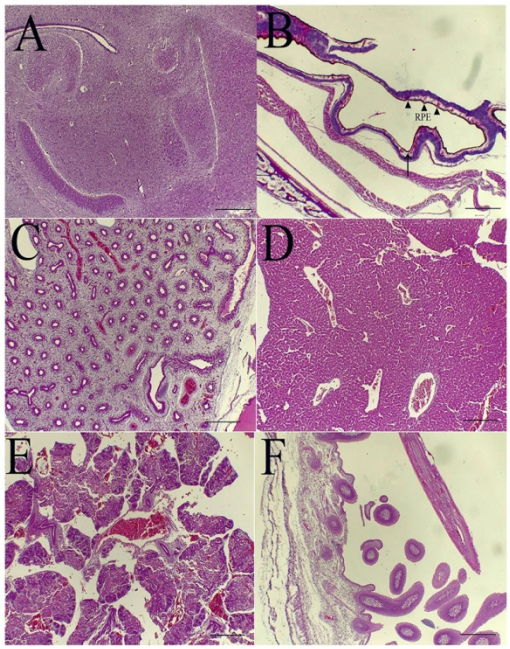

Figure 3(D)

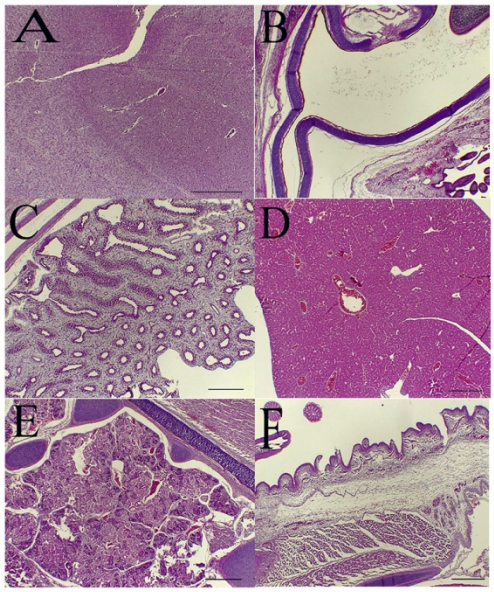

Figure 3(E)

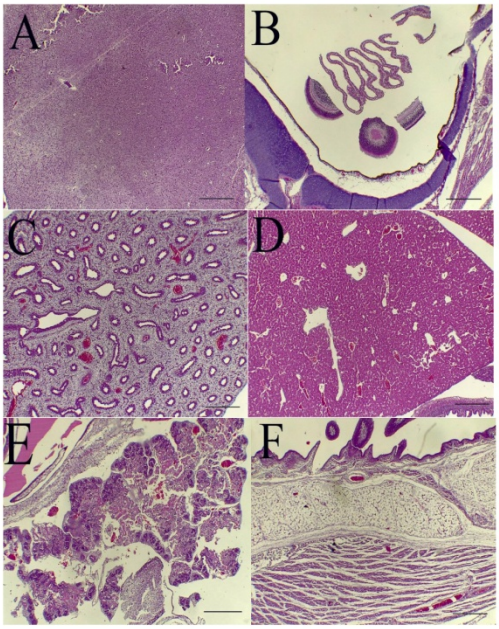

Figure 3(F)

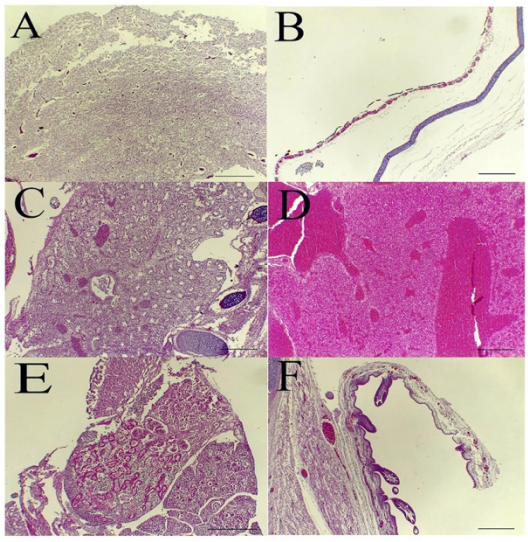

Figure 3(G)

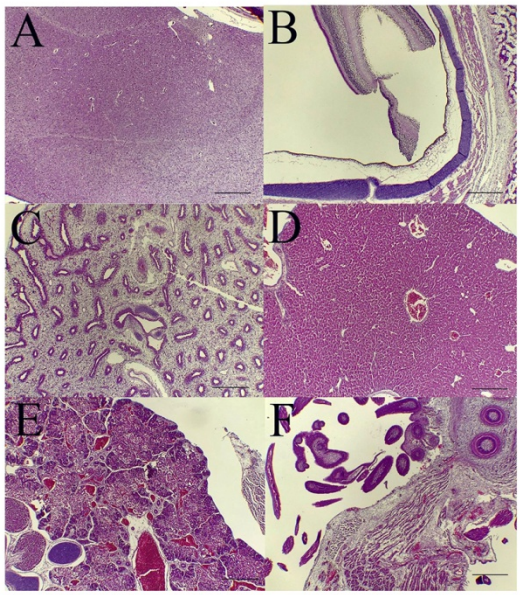

Figure 4

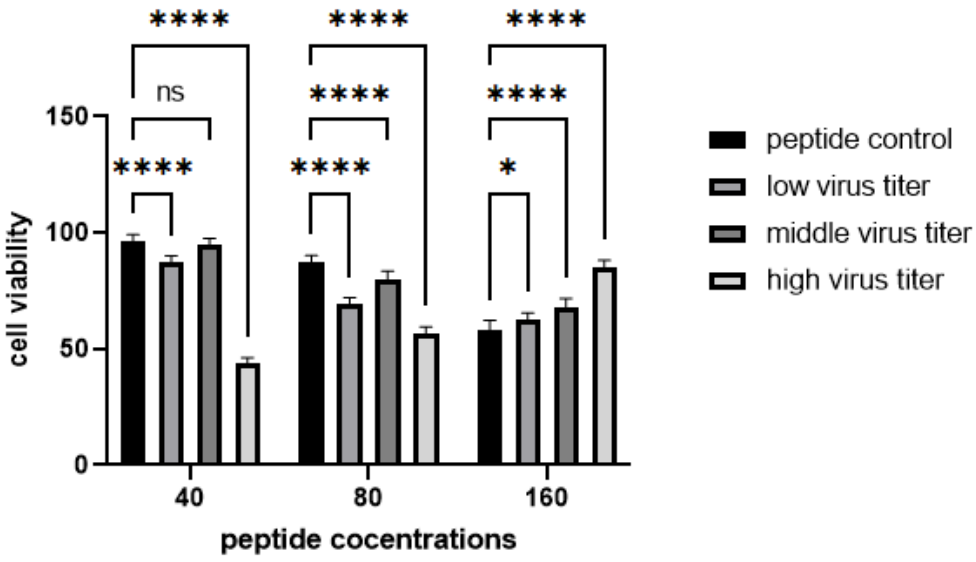
****
****
****
ns
****
****
****
****
*
150
100
50
0
cell viability
40
80
160
peptide cocentrations
peptide control
low virus titer
middle virus titer
high virus titer

Figure 5(A)

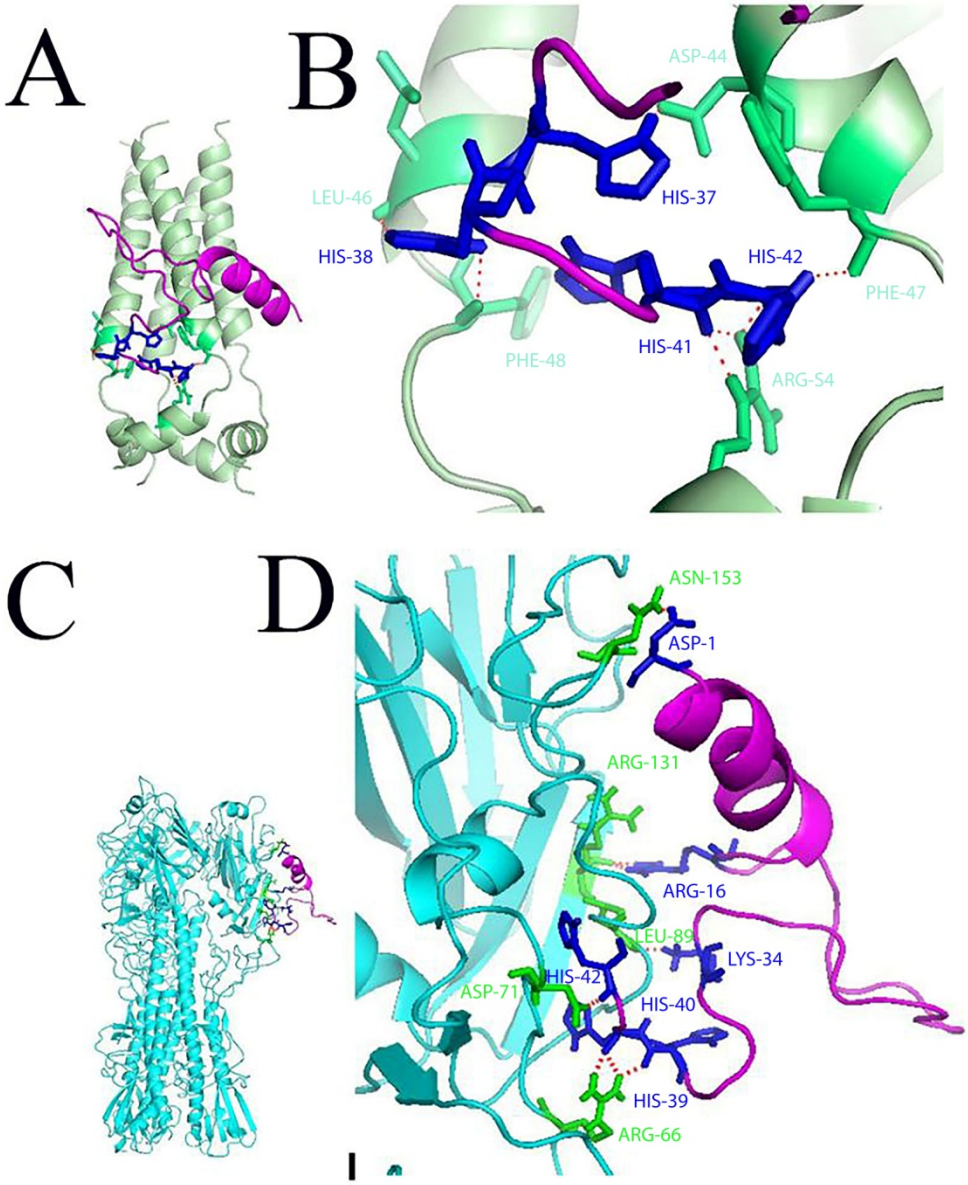
A
B
ASP-44
LEU-46
HIS-37
HIS-38
HIS-42
PHE-47
HIS-41
PHE-48
ARG-S4
C
D
ASN-153
ASP-1
ARG-131
ARG-16
LEU-89
LYS-34
HIS-42
ASP-71
HIS-40
HIS-39
ARG-66

Figure 5(B)

E F

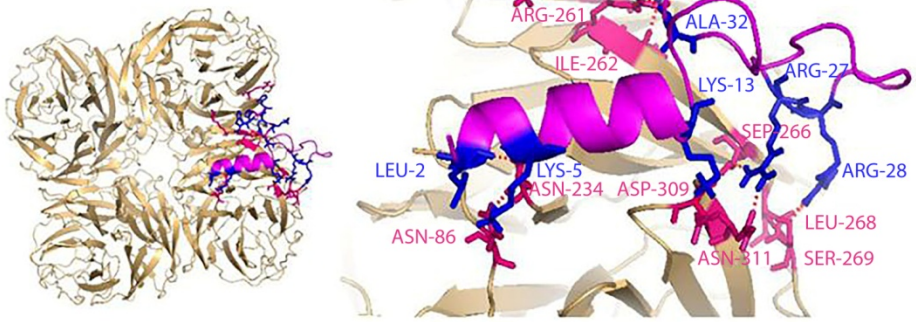
ARG-93
HIS-38
HIS-41
SER-450
LYS-34
HIS-42
LYS-415
HIS-37
ARG-261
ALA-32
ILE-262
ARG-27
LYS-13
SEP-266
LEU-2
LYS-5
ARG-28
ASN-234
ASP-309
LEU-268
ASN-86
ASN-311
SER-269